

Vol.13, No.3, July-September 2025, 256-265

PSO-Optimized Power Allocation in NOMA-QAM for Beyond 5G: A CFD and MFD Analysis

Jaspreet Kaur^{1*}

1. Institute of Engineering and Technology, Lucknow

Received: 20 Sep 2024/ Revised: 04 Sep 2025/ Accepted: 05 Oct 2025

Abstract

This paper proposes a power allocation method based on particle swarm optimization (PSO) to enhance spectrum sensing performance in downlink Non Orthogonal Multiple Access (NOMA) systems employing high-order Quadrature Amplitude modulation (QAM) modulation for beyond 5G networks. By intelligently adjusting user power levels, the proposed approach significantly improves detection reliability while maintaining stringent false alarm constraints, even under challenging low-SNR conditions. The goal is to enhance spectrum sensing performance by maximizing the probability of detection (P_d) while maintaining a constrained probability of false alarm (P_f). Cyclostationary Feature Detection (CFD) and Matched Filter Detection (MFD) techniques are applied to evaluate detection performance under varying Signal to noise ratio (SNR) conditions. Simulation results demonstrate that the optimized framework not only strengthens detection performance particularly for high order QAM but also enhances overall system responsiveness. Also CFD surpasses MFD in higher SNR scenarios due to its ability to exploit cyclic features of modulated signals, which are preserved even in moderately noisy environments. The integration of PSO further enhances system performance, offering a practical and scalable solution for next-generation Internet of Things (IoT)-enabled spectrum sharing environments.

Keywords: Non Orthogonal Multiple Access (NOMA); Matched Filter Detection (MFD); CFD, PSO; Cognitive Radio Networks (CRN); Next Generation Networks (NGN).

1- Introduction

The increase in the number of connected devices and the rapid expansion of wireless services are creating an unprecedented need for spectral resources, pushing networks toward the capabilities envisioned for beyond 5G and 6G systems [1]. Because cognitive radio (CR) technology allows for dynamic spectrum access and opportunistic usage of unused frequency bands, it has become a key paradigm to solve spectrum shortages [2]. NOMA has simultaneously become well-known as a crucial method for enhancing spectral efficiency and facilitating huge connections [3-4]. CR employs three primary sensing methods to detect available spectrum: Energy Detection (ED), Matched Filter Detection (MFD), and Cyclostationary Feature Detection (CFD). It has been found in recent surveys that over 75% of spectrum is wasteful [4]. Therefore, it is crucial to make use of unutilized spectrum. Primary users (PUs) possessing license do not always use the allocated spectrum, causing spectrum to be wasted. Assigning spectrum to unlicensed users, frequently referred to as secondary users or SU, is one method of increasing spectrum utilization when PUs are discovered to be inactive [5]. Simultaneously, the spectrum ought to be redistributed to the PUs whenever they choose to utilize it, without affecting the SU's performance [6]. This implies that SUs should use the spectrum whether or not PUs are present. There is great potential for attaining high data rates and effective spectrum usage when CR and NOMA are combined, especially when using high order modulation techniques like 64-QAM and 256-QAM [7-8]. These benefits, however, come at the expense of more complicated spectrum sensing and a greater susceptibility to fading and noise, particularly in the low signal-to-noise ratio (SNR) conditions typical of CR situations [9]. For secondary users to operate dependably in shared spectrum scenarios and to prevent detrimental interference with primary users, accurate spectrum sensing is necessary [10]. This study addresses the central question of whether an intelligent power allocation strategy can enhance spectrum sensing performance in CR-enabled NOMA

systems while maintaining strict constraints on false alarm rates. We hypothesize that a Particle Swarm Optimization (PSO)-based approach can dynamically allocate user power in a manner that maximizes detection probability, reduces sensing time, and maintains efficient spectrum utilization even under challenging conditions. Conventional sensing techniques, including CFD and MFD, often exhibit degraded performance in low SNR conditions, particularly when dealing with high-order modulations [11-12]. Moreover, many existing studies focus solely on detection algorithms without considering adaptive resource allocation as part of the sensing framework. Our work bridges this gap by integrating PSO-based power optimization into the CR-NOMA sensing process, offering a holistic solution that jointly considers sensing accuracy and power efficiency. This represents a substantial contribution toward enabling practical, robust CR-NOMA implementations. The motivation for this research lies in the growing demand for agile and energy-efficient spectrum sharing techniques capable of supporting high-throughput applications, Internet of Things (IoT) deployments, and massive machine-type communications. By optimizing power allocation, we aim to achieve reliable detection performance without excessive sensing overhead, paving the way for practical deployment of cognitive radio systems in next-generation networks. Motivated by the need for improved detection in noisy NOMA-QAM environments, this work proposes a PSO-based power allocation framework to enhance spectrum sensing performance. Key contributions include:

- (i) Development of a PSO-optimized power allocation scheme for NOMA systems with high-order QAM to boost detection accuracy.
- (ii) Comparative analysis of CFD and MFD for QAM-64 and QAM-256 modulation schemes.
- (iii) Simulation results showing up to 47.91% improvement in detection probability (Pd) over conventional MFD, validating the approach in challenging noise conditions.

This is how the rest of the paper is structured. Relevant literature related to NOMA, QAM, MFD, CFD and PSO is given in Section 2. The system model and the suggested PSO-based optimization methodology are covered in depth in Section 3. Simulation data, performance comparisons, and information on the efficacy of the suggested strategy are presented in Section 4. The paper's conclusion and some future study directions are covered in Section 5 and 6.

2- Literature Review

Lately, a number of research on spectrum sensing techniques using NOMA demonstrated potential in fulfilling the spectrum needs of several 5G applications. 5G mobile communications are about to become worldwide. For an OFDM system, cyclic prefix detection was proposed by Arun et al. [13]. The recommended method's demand for previous knowledge from the principal user is one of its key drawbacks. The energy detection method of SS for OFDM system was implemented by the authors [14]. The simulation results show that while OFDM without CP performs better towards P_f, OFDM system consisting of CP shows improved throughput performance. Recent studies further extended the applicability of NOMA-based cognitive systems [21-22]. Recent advancements in spectrum sharing and NOMA integration have focused on intelligent resource allocation and IRS-assisted systems to enhance performance in Beyond 5G networks [25-26]. Additionally, Bala Kumar and Nanda Kumar [28] explored block chain-enabled cooperative spectrum sensing in MIMO-NOMA CRNs for improved security and sensing accuracy. For instance, Salameh et al. [29] feature-based spectrum sensing to adaptively detect primary user signals in fading channels without requiring a fixed detection threshold while Zhai et al. [30] proposed a joint optimization scheme combining active IRS and multicluster NOMA to improve spectral efficiency. These works underscore a growing trend toward intelligent, adaptive spectrum management strategies. However, most of these approaches either focus on physical-layer improvements or overlook sensing complexity under high-order modulation and low-SNR conditions. In contrast, this study addresses the need for efficient spectrum sensing by integrating PSO-based power allocation with advanced detection techniques in high-QAM NOMA-CR systems. Detailed literature specifically for NOMA-QAM systems is given in Table 1.

S.No Reference Year Aim **Findings** Implementation and analysis done 2010 [15] Implement and examine a MIMO-OFDM system using MATLAB simulations 3 dB gain with optimized NOMA 3 [4] 2019 Enhance sensor performance at low SNR over O-NOMA NOMA-CRN outperforms Explore advanced spectral efficiency techniques in CRNs 2019 4 [1] conventional CR in spectrum using NOMA and 5G signals. efficiency To Integrate NOMA into CR networks to enhance spectrum High SE and large user support 5 2020 [3] efficiency and accommodate large number of users shown in CR scenarios Allows SU to use several PU types with and without 6 [22] 2021 Use NOMA to efficiently utilize the spectrum interference Weak user power boost improves To Assess the effectiveness of NOMA in uplink 7 2021 performance, especially at low [24] communications using fixed power coefficients. **SNRs** SI types classified; challenges and 8 2021 [27] Apply Swarm Intelligence to address future network issues research opportunities discussed Cyclostationary methods show 2 dB advantage over traditional [26] 2022 Detailed review of 5G waveforms using sensing methods techniques Demonstrated enhanced security Introduce block chain-enabled cooperative and reliability in spectrum sensing 10 [28] 2024 spectrum sensing for 5G/B5G CR using using decentralized block chain massive MIMO-NOMA mechanisms in MIMO-NOMA

Machine learning-driven, feature-based spectrum sensing

approach to improve NOMA signal detection in dynamic IoT

networks operating under fading channels.

Table 1 :- Literature Review relevant to proposed Work

2-1- Research Gap and Motivation

[29]

2025

11

Despite the extensive efforts to enhance spectrum efficiency using CR and NOMA techniques, several challenges remain unaddressed. Most of the prior works focus on static or suboptimal power allocation strategies, often overlooking the impact of dynamic power tuning under high-order modulation schemes. Furthermore, few studies have explored the integration of advanced optimization algorithms such as swarm intelligence for real-time adaptation in CR-NOMA environments under low-SNR conditions. Additionally, limited work has been done to jointly optimize sensing accuracy and power distribution while accounting for false alarm constraints in high-QAM signal environments. As a result, a critical gap persists in developing unified frameworks that can adaptively optimize both detection performance and

spectral efficiency in practical CR scenarios. Motivated by this gap, the present study proposes a novel power allocation framework based on Particle Swarm Optimization (PSO), tailored for CR-enabled NOMA systems operating under high-order QAM. The approach aims to achieve enhanced sensing accuracy, reduced false alarm rates, and optimized throughput, all while maintaining practical feasibility for next-generation wireless systems.

CRNs.

Method Employs feature-based

spectrum sensing to adaptively

detect primary user signals in fading channels without requiring

a fixed detection threshold.

3- Proposed System Model

This work investigates a downlink NOMA-based communication system utilizing QAM modulation for Beyond 5G scenarios. Multiple users are multiplexed in the power domain and served concurrently over a shared channel. Power levels for each user are dynamically

allocated using Particle Swarm Optimization (PSO) to enhance overall detection performance while maintaining user fairness. At the receiver, spectrum sensing is carried out using both CFD and MFD, with performance evaluated across different SNR values for QAM-64 and QAM-256 schemes. The PSO algorithm optimizes power allocation by maximizing the $P_{\rm d}$ under a constraint on the

 $P_f \leq 0.5$. These methods help the CR identify when the spectrum is idle based on two hypotheses: H1(primary user presence) and H0(absence of a primary user).

Table 2.Comparison			

S. No.	Spectrum Sensing	Remarks
	Technique	
1	Conventional Energy	Simple to implement with low computational complexity.
	Detection	Poor performance at low SNR ($P_d = 0$ at SNR < -12 dB).
		Susceptible to interference be-tween PUs and SUs.
2	Conventional CFD	Robust detection at low SNR (Requires prior knowledge of signal periodicity).
		Moderate computational complexity due to autocorrelation.
3	Conventional MFD	Effective at low SNR ($P_d = 0.19$ at SNR = 4 dB for QAM-256).
		Requires prior knowledge of PU signal.
		SUs can only use spectrum in absence of PUs.
4	Proposed Optimized MFD	High P_d (0.83 at $P_f = 0.5$ for QAM-256, 47.91% improvement over MFD).
	& CFD	Robust at low SNR ($P_d = 0.79$ at SNR = -5 dB).
		Increased computational complexity due to PSO optimization.

3-1- Matched Filter Detection

The MFD technique evaluates whether primary users are present by comparing the detected signal with a reference signal. The next step involves comparing the output with a dynamic threshold. It is extremely effective in low SNR since it optimizes SNR in presence of AWGN. The formula for the test statistic is $TMF = \sum y(n) *x(n)$. The PU signal in this case is represented by (x), the SU signal by (n), and the test parameter for MFD is TMF. It then compares a threshold with the test statistics (TMF) to ascertain availability of spectrum. The signal received from Secondary and Primary user are roughly modeled as random Gaussian variables as depicted in fig. (1).

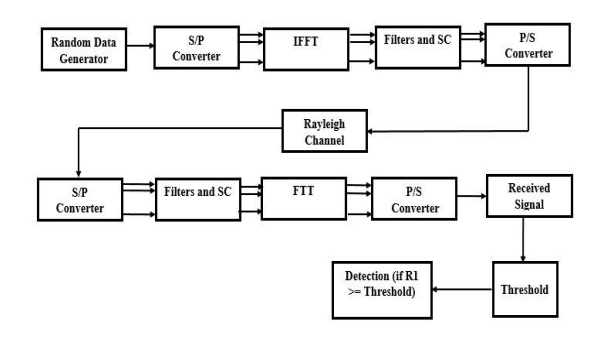


Figure 1. Block diagram for NOMA MFD

3-2- Cyclostationary Feature Detection

CFD is amongst the most significant technique for advanced as it is able to identify the spectrum at low SNR without the impact of noise. It uses signal's periodicity features as it calculates mean and autocorrelation of the signal. The spectrum correlation density functions and cyclic autocorrelation are useful in order to estimate the CS signals. The initial stage in CS is to use a number of procedures, including filtering, encoding, and sampling, to convert the signal into second-order CS.

$${y(+)} = {y(t + to)}$$
 (3)

The (r) is represented as cyclic auto-correlation function at:

$$\beta \gamma = \{M/T_0\} \tag{4}$$

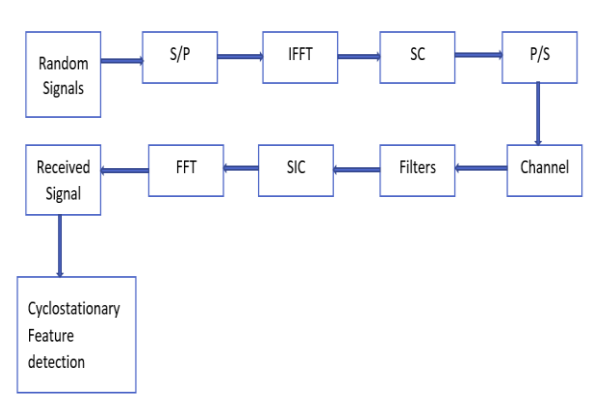


Figure 2. Block diagram for NOMA CFD

In a NOMA system, each subcarrier's power spectrum density (PSD) can be characterized. For n-th subcarrier, PSD can be represented as:

$$\varphi n(f) = PnTs \left(\frac{Sin\pi fTs}{\pi fTs}\right)^2 \tag{5}$$

where, T_s stands for the symbol duration, φ is the PSD of the next subcarrier, and P_n is transmit power that is

released by preceding subcarrier. A possible technique to represent CFD using NOMA is as

$$\varphi n(f) = |Hn(f)|^2 \tag{6}$$

The prototype filter's frequency spectrum with coefficient h[n] and n=0, 1... W-1 is represented as $H_n(f)$ [6]. An example of a frequency response's source is:

$$|\operatorname{Hn}(f)| = h\left[\frac{w}{2}\right] + 2\sum_{i=1}^{\frac{W}{2}-1} h\left[\left(\frac{w}{2}\right) 1\right] \cos(2\prod r) \tag{7}$$

The following formula determines the phase angle:

$$Ph(u) = [so^{u}, s1^{u}, s2^{u} \dots sl - 1^{u}]$$
 for u=1, 2...U

$$sj^{(u)} = exp(j\theta_0^{(u)})$$

j=0, 1, L-1, and where $j\theta_0^{(u)}$ denotes random phase angle. So the representation of NOMA symbol can be shown as:

$$Y_k = [Y_{k,0}, Y_{k,1} \dots \dots \dots \dots Y_{k,l-1}] (10)$$

The phase angle is applied to the NOMA symbols as follows:

$$\begin{split} Y_{k}^{(v)} &= p^{(u)} * Y_{k} & (11) \\ y^{u}(t) &= \sum_{I=0}^{L-1} \sum_{K=0}^{k-1} X_{k',I}^{(U_{min})} h(t - \frac{K'T}{2})) e^{\frac{j2\prod It}{T}} e^{j\Theta} K'I + \sum_{I=0}^{L-1} d_{k,I}^{(u)} h(t - \frac{KT}{2})) e^{\frac{j2\prod It}{T}} e^{j\Theta} K'I \end{split}$$

Lastly, the following represents the received NOMA signal:

$$Y'(t) = \sum_{k=0}^{K-1} X_{k',l}^{(U_{min})} e^{j\Theta_{k,l}} h(t - k^{R_0})$$
 (13)

We can infer from Eq. (13) that the NOMA - CR system is capacious than traditional OFDM system. The block diagram of the recommended technique is displayed in Fig. 2. A sequential generation process generates a random parallel symbol. IFFT is used to examine the signal in the time domain, and once it has been transmitted across a Rayleigh channel, SC permits many users to use the sub-channel. The receiver uses SIC to decode the time domain signal and FFT to translate it to the frequency domain. In the end, a threshold is determined and if received symbol's energy exceeds the threshold value, identification will occur; otherwise, no detection will be taken into account.

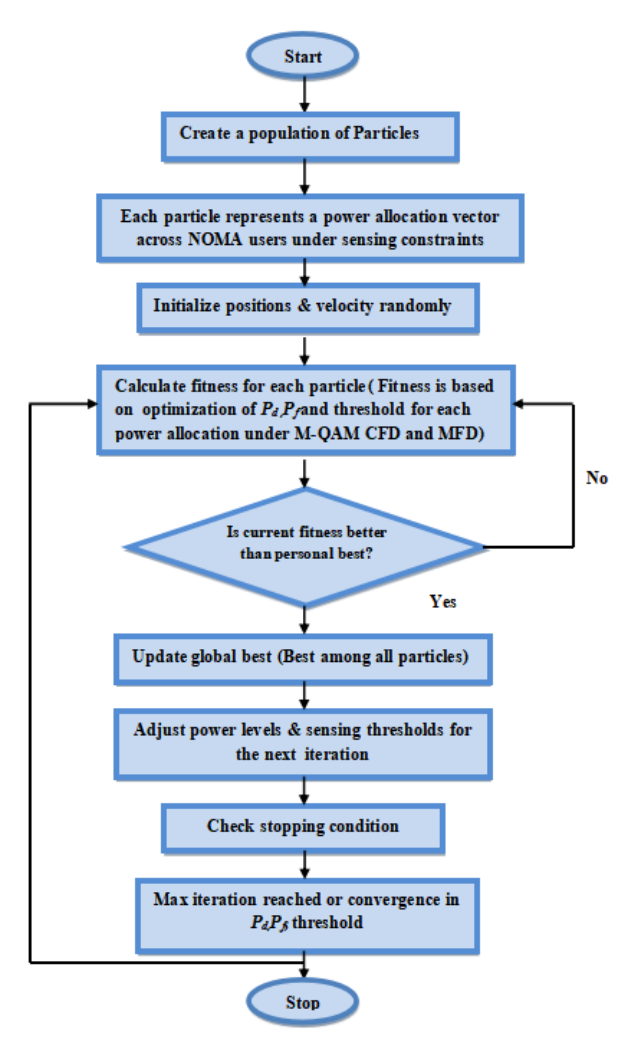


Figure 3. Flowchart of MFD and CFD Technique using PSO

4- Simulation Parameters and Performance Analysis.

In an effort to implement the suggested algorithm shown in Fig. 3 MATLAB 2022 is used. Table 3. depicts the simulation parameters for optimizing and analyzing NOMA QAM CFD and MFD using PSO. Simulation results of matched filter spectrum sensing method and Cyclostationary feature detection based on NOMA are used to comprehensively examine the results. This study determines the threshold value at the NOMA system's receiver end.

Table 3. Simulation Parameters

Parameters	Description	Values
f	frequency	16 MHz
M	QAM order	64,256
BW	Bandwidth	30 MHz
N	Number of users	50
n	Population size	100
SNR	Signal to noise ratio	-20dBto 5 dB
k	FFT Size	1024

It is based on the idea that only detection will be presumed if the signal received equals or exceeds the threshold value; otherwise, no detection will be inferred. When assessing the effectiveness of MFD and CFD, a constant threshold value is taken into account because a changing threshold can deteriorate the efficiency of spectrum sensing methods. To

investigate the role of thresholds in MFD and CFD identification, QAM-64 and QAM-256 transmission systems with 64 and 256 sub-carries were used. Table 4 and Figure 4 display the P_d for various P_f values. P_f indicates the false representation of noise as a desired signal. SNR = 10 dB was fixed in the current simulation to analyze the effectiveness of MFD & CFD strategy for NOMA. It is seen from fig.4 and table 4 that NOMA M-256 P_d is higher than M-64. So it is inferred that NOMA-QAM-MFD 256 Pd is better than QAM-64 as shown in fig (4).

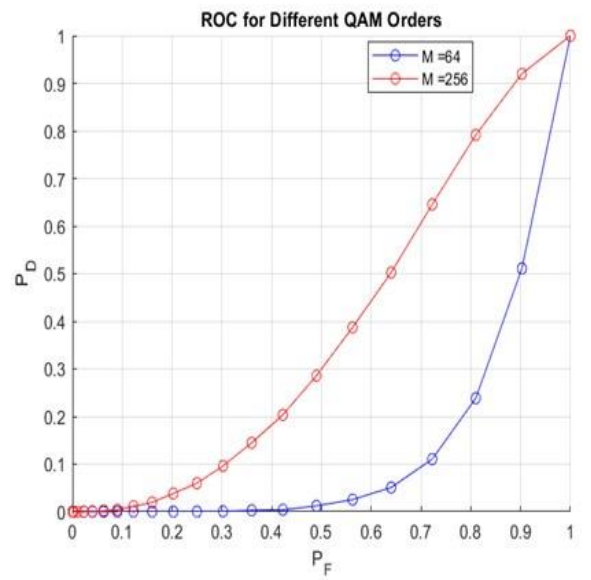


Figure 4: P_d Vs P_f for M-QAM MFD

Table 4: NOMA-QAM MFD Pd vs Pf result

P _f /P _d (MFD)	0.1	0.2	0.3	0.4	0.6	0.7	0.8	0.9	1
NOMA M-256	0	0	0	0.07	0.14	0.27	0.47	0.76	1
NOMA M-64	0	0	0	0.05	0.09	0.18	0.33	0.56	1

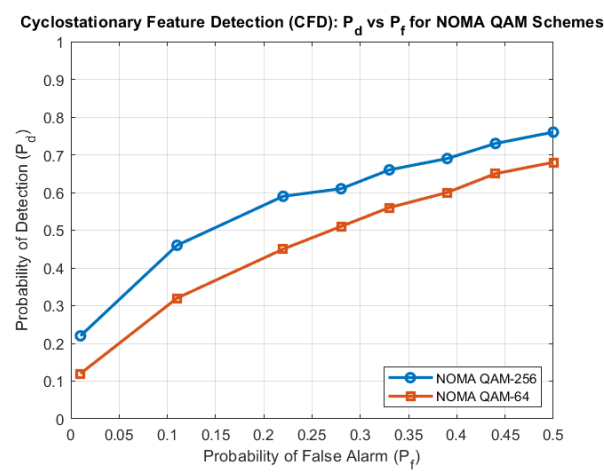


Figure.5. Pd Vs Pf for CFD for M-QAM.

Table 5: Pd vs Pf for NOMA-QAM using CFD

P _f /P _d (CFD)	0.01	0.11	0.22	0.28	0.33	0.39	0.44	0.50
NOMA QAM- 256	0.22	0.46	0.59	0.61	0.66	0.69	0.73	0.76
NOMA QAM- 64	0.12	0.32	0.45	0.51	0.56	0.60	0.65	0.68

Table 5 and Figure 5 shows the Pd vs Pf values for M-QAM CFD. A comparative analysis demonstrates the clear advantage of the proposed NOMA-CFD approach over MFD. At Pf = 0.5 and SNR = 10 dB, CFD with QAM-256 achieves a Pd of 0.76, outperforming both QAM-64 (Pd = 0.68) and MFD, with an observed 44.28% improvement in detection probability. Across the full range of Pf values, CFD consistently maintains higher Pd, indicating superior sensing reliability and robustness to false alarms compared to conventional techniques.

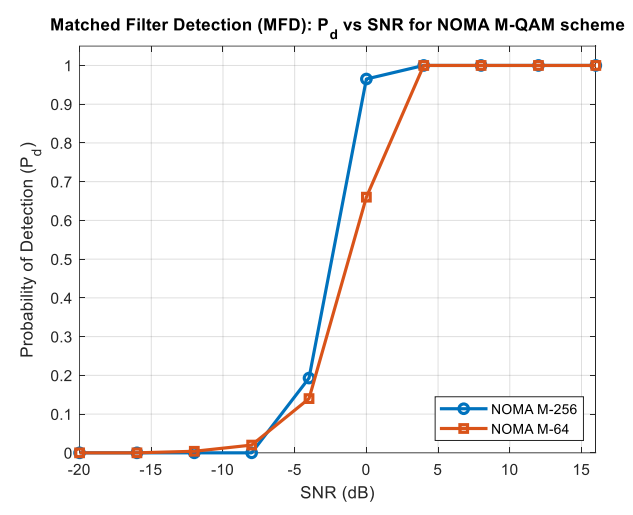


Figure 6. Plot for MFD Pd against SNR.

	Table 6. P _d against SNR for MFD in NOMA-QAM												
SNR/Pd	-	-	-12	-8	-4	0	4	8	12	16			
(MFD)	20	16											
NOMA	0	0	0	0	0.19	0.965	1	1	1	1			
M-256													
NOMA	0	0	0.004	0.02	0.14	0.66	1	1	1	1			

The Pd is displayed as a function of SNR in Table 6 and Fig.6. We do analysis and simulations across a variety of SNR values (10 dB to 20 dB) for MFD. For QAM-64 & 256, 100% Probability of detection (Pd) is achieved at 4 dB and 6 dB, respectively. Therefore, QAM-Pd can be considered better than QAM-256. For instance, at SNR = -10 dB, MFD yields a Pd of 0.56 (QAM-256), while CFD fails to detect (Pd \approx 0). However, at SNR = 4 dB, CFD rapidly improves to Pd = 1.0, outperforming MFD's Pd of

0.97. This demonstrates CFD's steeper gain in detection performance once the SNR threshold is crossed.

Table 6 and Figure 6 shows the Pd for various Pf values. SNR = 10 dB was fixed in the current simulation to measure the effectiveness of the CFD strategy for NOMA. It is seen that for NOMA QAM CFD Pd value is 0.76 for Pf of 0.50 as compared to 0.68 Pd value for NOMA QAM-64. Also

Table 7.Pd vs SNR for NOMA-QAM with CFD

SNR(dB)/P d	-25	-20	-15	-10	-5	0	+5
NOMA QAM-256	0.1 1	0.1 6	0.3	0.5 6	0.7 9	0.9 7	1
NOMA QAM-64	0.1	0.1 5	0.3	0.5 0	0.7 4	0.9 1	0.9 8

Tab	ole 8.	BER	vs S	SNR	of :	NO	MA	۱-QA	М	MFD	&	CFD	į
-----	--------	-----	------	-----	------	----	----	------	---	-----	---	-----	---

P_f/P_d	0.0	0.0	0.1	0.1	0.2	0.2	0.3	0.4	0.5
	1	6		5		5			0
Optimiz	0.3	0.3	0.3	0.4	0.4	0.4	0.4	0.4	0.4
ed P _d of	3	7	9	0	2	3	5	7	9
MFD									
Optimiz	0.5	0.5	0.6	0.7	0.7	0.7	0.7	0.8	0.8
ed P _d of	1	9	3	0	3	5	9	1	3
CFD									

results improve by 44.28% when compared with MFD technique. The figure illustrates that NOMA-QAM-256 P_d is better than QAM-64. Also it is clear from results that NOMA-CFD outperforms the results of MFD.

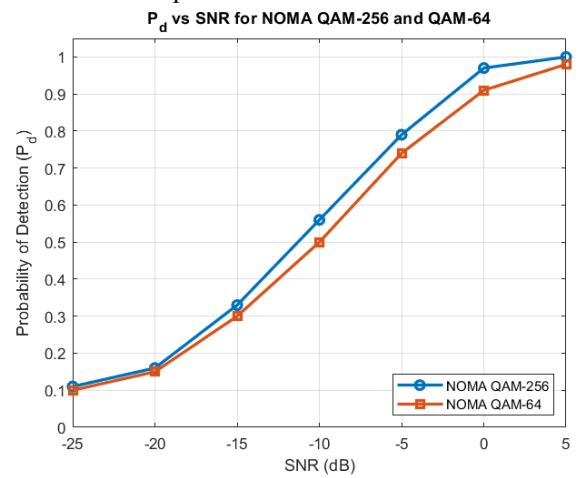


Figure.7. Pd Vs SNR for CFD.

The table 7 and Fig. 7 depicts results of P_d vs SNR of NOMA-QAM CFD. We examine and model P_d throughout a spectrum of SNR ranging from -25 to 5dB. From obtained results it is evident that at 0 dB and 5dB in the case of QAM-64 and QAM-256, P_d reaches an ideal value of 100%. Thus, it may be said that QAM- 64 Pd is superior to QAM-256's. The superior low-SNR performance of MFD is due to its reliance on known signal templates. In contrast, CFD requires stronger signals to detect Cyclostationary features but eventually surpasses MFD in higher-SNR regions,

making it better suited for mid-to-high-SNR cognitive environments.

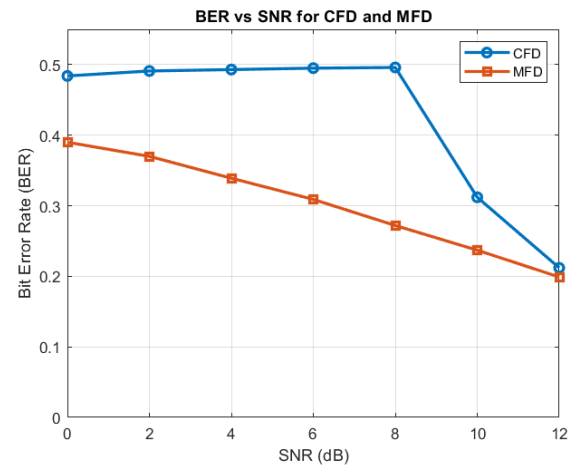


Figure 8. BER vs SNR of NOMA-QAM MFD & CFD

As SNR increases, the BER lowers, as Fig. 8 and Table 8 demonstrate. For M-256, a BER of 0.309 is obtained at 6 dB using the MFD technique and 0.212 at 12 dB using the CFD technique. Matched Filter Detection MFD consistently achieves lower BER compared to CFD across all SNR levels due to its reliance on known signal patterns. CFD shows limited improvement at low SNR but performs better as SNR increases beyond 10 dB. Overall, MFD is more reliable for low-SNR environments, while CFD requires stronger signals to reduce errors.

Figure 8 reinforces these findings, showing that MFD achieves a BER of 0.309 at 6 dB, while CFD only achieves 0.212 at 12 dB. This indicates that while MFD offers lower BER in noisy environments, CFD benefits more from clean conditions. As observed in Tables 5 and 7, Pd increases with SNR for both MFD and CFD. Notably, MFD achieves a Pd of 0.97 at 0 dB for QAM-256, while CFD reaches similar performance only at higher SNR levels (>4 dB). This indicates that MFD is more suitable for low-SNR environments due to its coherent detection mechanism.

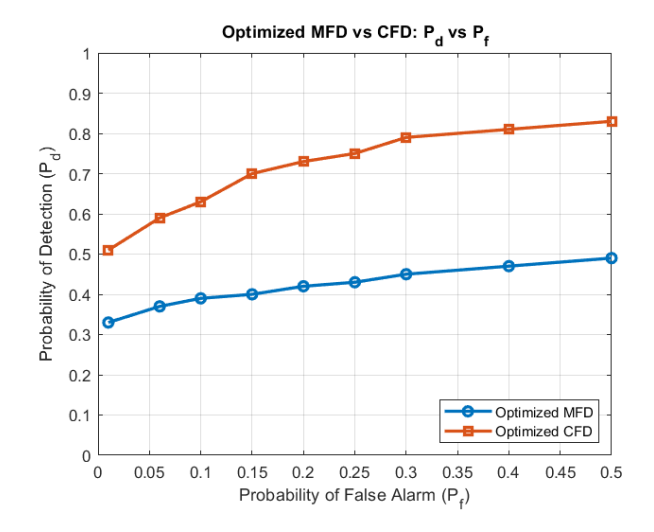


Figure 9. Optimized Pd using MFD and CFD using PSO

Table 9. Pf against optimized Pd using PSO for CFD in NOMA-QAM

	. I I again						
BER							
of							
CFD	0.484	0.491	0.493	0.495	0.496	0.312	0.212
BER							
of							
MFD	0.39	0.37	0.339	0.309	0.272	0.237	0.199
SNR	0	2	4	6	8	10	12

Table 9 and Fig. 9 shows PSO-optimized Pd vs Pf plot using PSO in MFD and CFD technique. Results improved and high value of Pd was achieved for lesser Pf values showing improved detection performance (Pd of 0.75) at reduced false alarm rates (P_f of 0.33). At $P_f = 0.3$, PSO-optimized CFD achieves $P_d = 0.79$, which translates to a 35% increase in successful PU detection compared to MFD. This is critical in CR-IoT applications where minimizing missed detection reduces interference and improves network reliability. CFD surpasses MFD in higher SNR scenarios due to its ability to exploit cyclic features of modulated signals, which are preserved even in moderately noisy environments. The integration of PSO further enhances detection performance by adaptively selecting parameters that maximize P_d under false alarm constraints. Despite its superior performance, CFD exhibits higher computational complexity compared to MFD, making it less suitable for real-time or resource-constrained IoT nodes. Additionally, requires tuning and incurs optimization overhead, which may limit deployment in ultra-low-latency scenarios.

5- Conclusion

This study introduces a PSO-optimized power allocation framework for NOMA-QAM systems in cognitive radio environments, targeting enhanced detection using CFD and MFD techniques. The proposed model significantly

improves detection performance, particularly for high-order modulation schemes like QAM-256, achieving up to 47.91% gain in P_d over traditional MFD approaches. CFD demonstrates superior robustness at low SNR and reduced sensing time when optimized via PSO. These improvements contribute to more reliable and energy-efficient spectrum access, addressing the demands of IoT-enabled Beyond 5G networks. Future work will explore integration with IRS-assisted channels and deep learning-based sensing optimization for dynamic environments.

6- Future Research Directions

Future research can extend the proposed PSO-based power allocation framework to support advanced modulation schemes like OFDM and OTFS. Incorporating adaptive sensing techniques, such as machine learning-based threshold selection or reinforcement learning, may further enhance detection in dynamic environments. Additionally, integrating Intelligent Reflecting Surfaces (IRS) to improve signal quality and spectral efficiency, especially in obstructed scenarios, is a promising direction. Finally, validating the system's scalability in large-scale IoT deployments and testing it on real-world platforms would strengthen its practical relevance.

References

- [1] Kumar, A., Bharti, S., & Gupta, M. (2019). FBMC vs. OFDM: 5G mobile communication system. International Journal of Systems, Control and Communications, 10(3), 250-264. DOI:10.5815/ijwmt.2023.05.01
- [2] Haykin, S., Thomson, D. J., & Reed, J. H. (2009). Spectrum sensing for cognitive radio. Proceedings of the IEEE, 97(5), 849-877. DOI:10.1109/JPROC.2009.2015711
- [3] Kumar, Arun, et al. "NOMA based CR for qam-64 and qam-256." Egyptian Informatics Journal 21.2 (2020): 67-71. DOI:10.5815/ijwmt.2023.05.01
- [4] Kumar, Arun, and P. Nandha Kumar. "OFDM system with Cyclostationary feature detection spectrum sensing." ICTExpress 5.1 (2019): 21-25. DOI:10.1016/j.icte.2018.01.007
- [5] Liang, Y. C., Chen, K. C., Li, G. Y., & Mahonen, P. (2011). Cognitive radio networking and communications: An overview. IEEE transactions on vehicular technology, 60(7), 3386-3407. DOI: 10.1109/TVT.2011.2158673
- [6] Datla, D., Wyglinski, A. M., & Minden, G. J. (2009). A spectrum surveying framework for dynamic spectrum access networks. IEEE [7]Transactions on Vehicular Technology, 58(8), 4158-4168. DOI: 10.1109/TVT.2009.2025380
- [8]Goldsmith, A., Jafar, S. A., Maric, I., & Srinivasa, S. (2009). Breaking spectrum gridlock with cognitive radios: An information theoretic perspective. Proceedings of the IEEE, 97(5), 894-914. DOI: 10.1109/JPROC.2009.2015717
- [9] Tumuluru, V. K., Wang, P., & Niyato, D. (2011). A novel spectrum-scheduling scheme for multichannel cognitive radio network and performance analysis. IEEE Transactions on

- Vehicular Technology, 60(4), 1849-1858. DOI: 10.1109/TVT.2011.2117951
- [10] Navrátil, P. A., Childs, H., Fussell, D. S., & Lin, C. (2013). Exploring the spectrum of dynamic scheduling algorithms for scalable distributed-memoryray tracing. IEEE transactions on visualization and computer graphics, 20(6), 893-906. DOI: 10.1109/TVCG.2013.261
- [11] Nandhakumar, P., & Kumar, A. (2016). Analysis of OFDM system with energy detection spectrum sensing. Indian J. Sci. Technol, 9(16), 1-6. DOI: 10.17485/ijst/2016/v9i16/92224
- [12] Saberali, S. A., & Beaulieu, N. C. (2014, October). Matched-filter detection of the presence of MPSK signals. In 2014 International Symposium on Information Theory and its Applications (pp. 85-89). IEEE.DOI:0.1109/ISITA.2014.7001426
- [13] Kim, K., Akbar, I. A., Bae, K. K., Um, J. S., Spooner, C. M., & Reed, J. H. (2007, April). Cyclostationary approaches to signal detection and classification in cognitive radio. In 2007 2nd IEEE international symposium on new frontiers in dynamic spectrum access networks (pp. 212-215). IEEE. DOI: 10.1109/DYSPAN.2007.39.
- [14] Akyildiz, I. F., Lee, W. Y., Vuran, M. C., & Mohanty, S. (2006). NeXt generation/dynamic spectrum access/cognitive radio wireless networks: A survey. Computer networks, 50(13), 2127-2159. DOI: 10.1016/j.comnet.2006.05.001.
- [15] Tu, C. C., & Champagne, B. (2009). Subspace-based blind channel estimation for MIMO-OFDM systems with reduced time averaging. IEEE Transactions on Vehicular Technology, 59(3), 1539-1544.DOI: 10.1109/TVT.2009.2036728.
- [16] Zhou, Y., Wang, Y., Wang, T., Zhang, K., & Zhang, W. (2011, May). Iterative inter-cell interference coordination in MU-MIMO systems. In 2011 IEEE 73rd Vehicular Technology Conference (VTC Spring) (pp. 1-5). IEEE. DOI: 10.1109/VETECS.2011.5956799.
- [17] Andrews, J. G., Buzzi, S., Choi, W., Hanly, S. V., Lozano, A., Soong, A. C., & Zhang, J. C. (2014). What will 5G be?. IEEE Journal on selected areas in communications, 32(6), 1065-1082. DOI: 10.1109/JSAC.2014.2328098
- [18] Srinu, S., & Sabat, S. L. (2013). Cooperative wideband sensing based on cyclostationary features with multiple malicious user elimination. AEU-International Journal of Electronics and Communications, 67(8), 702-707. DOI: 10.1016/j.aeue.2013.01.002.
- [19] Quan, Z., Cui, S., Sayed, A. H., & Poor, H. V. (2008). Optimal multiband joint detection for spectrum sensing in cognitive radio networks. IEEE transactions on signal processing, 57(3), 1128-1140. DOI: 10.1109/TSP.2008.2008540.
- [20] Na, D., & Choi, K. (2019). DFT spreading-based low PAPR FBMC with embedded side information. IEEE Transactions on Communications, 68(3), 1731-1745. DOI: 10.1109/TCOMM.2019.2952549.
- [21] He, Z., Zhou, L., Chen, Y., & Ling, X. (2018). Low-complexity PTS scheme for PAPR reduction in FBMC-OQAM systems. IEEE Communications Letters, 22(11), 2322-2325. DOI: 10.1109/LCOMM.2018.2863908.
- [22] Kumar, A., & Gupta, M. (2018). A review on activities of fifth generation mobile communication system. Alexandria Engineering Journal, 57(2), 1125-1135. DOI: 10.1016/j.aej.2017.06.014.

- [23] Bairagi, A. K., et al. (2020). Coexistence mechanism between eMBB and uRLLC in 5G wireless networks. IEEE transactions on communications, 69(3), 1736-1749. DOI: 10.1109/TCOMM.2020.3046635.
- [24] Mounir, M., et al. (2021). A novel hybrid precoding-companding technique for peak-to-average power ratio reduction in 5G and beyond. Sensors, 21(4), 1410. DOI: 10.3390/s21041410
- [25] Kumar, A., et al. (2021). An Efficient Hybrid PAPR Reduction for 5G NOMA-FBMC Waveforms. Computers, Materials & Continua, 69(3). DOI: 10.32604/cmc.2021.019092
- [26] Miah, M. S., Schukat, M., & Barrett, E. (2020). Sensing and throughput analysis of a MU-MIMO based cognitive radio scheme for the Internet of Things. Computer communications, 154, 442-454. DOI: 10.1016/j.comcom.2020.02.040
- [27] Ramamoorthy, R., et al. (2022). Analysis of cognitive radio for Ite and 5g waveforms. Computer Systems Science & Engineering, 43(3).DOI: 10.32604/csse.2022.019943.
- [28] Pham, Q. V., et al. (2021). Swarm intelligence for next-generation networks: Recent advances and applications. Journal of Network and Computer Applications, 191, 103141. DOI: 10.1016/j.jnca.2021.103141.
- [29] Bala Kumar, D., & Nanda Kumar, S. (2024). Block chainenabled cooperative spectrum sensing in 5G and B5G cognitive radio via massive multiple-input multiple-output non orthogonal multiple access. Results in Engineering, 24, 102840.DOI: 10.1016/j.rineng.2024.102840
- [30] Salameh, H. B., & Hussienat, A. (2025). ML-Driven Feature-Based Spectrum Sensing for NOMA Signal Detection in Spectrum-agile IoT Networks under Fading Channels. IEEE Sensors Journal. DOI: 10.1109/JSEN.2025.3524968.
- [31] Zhai, Q., Dong, L., Cheng, W., Li, Y., & Liu, P. (2023). Joint optimization for active IRS-aided multicluster NOMA systems. IEEE Systems Journal, 17(4), 6691-6694. DOI: 10.1109/JSYST.2022.3228965.